

# Gerchberg–Saxton algorithm: experimental realisation and modification for the problem of formation of multimode laser beams

I.V. Il'ina, T.Yu. Cherezova, A.V. Kudryashov

**Abstract.** An original method is proposed to calculate the formation of specified far-field intensity distributions by a bimorph mirror in the case of initial transverse-multimode beams. The method is based on the Gerchberg–Saxton algorithm with replacement of the phase function in the plane of the control element by a function that takes into account both the intensity and phase distributions of each mode. The numerical results on the formation of a beam with the third-order super-Gaussian intensity distribution from beams composed of two or four lowest transverse modes are discussed. The experimental results on using the conventional Gerchberg–Saxton algorithm to form a desired intensity distribution from single-mode laser beams using a liquid-crystal modulator are presented.

**Keywords:** Gerchberg–Saxton algorithm, formation of a specified laser intensity distribution, bimorph mirror, liquid crystal modulator.

## 1. Introduction

The wide use of lasers in modern industrial technologies (laser processing, lithography, and printing) [1, 2], medicine [3], and chemistry [4, 5], as well as in navigation, information, and location systems [6], put in the forefront the problem of optimisation of laser radiation parameters. The requirements imposed on laser radiation can be greatly different depending on a particular problem. For example, metal cutting requires, as a rule, tight focusing of a laser beam on the metal surface [7]. The main condition for laser thermal processing of materials is the uniform intensity distribution over the beam cross section [8]. In addition, because the laser radiation power is an important factor for the possibility and efficiency of such technological processes, it is often preferable to use multimode lasers. Thus, the control of the spatial structure (i.e., of the intensity profile) of multimode laser radiation is of particular practical interest.

I.V. Il'ina, T.Yu. Cherezova Department of Physics, M.V. Lomonosov Moscow State University, Vorob'evy gory, 119991 Moscow, Russia; e-mail: cherezova@mail.ru;

A.V. Kudryashov Moscow State Open University, Shatura branch, ul. Sportivnaya 9, 140700 Shatura, Moscow region, Russia; e-mail: kud@activeoptics.ru

Received 14 March 2008; revision received 10 November 2008

Kvantovaya Elektronika 39 (6) 521–527 (2009)

Translated by M.N. Basieva

One of the most widespread methods for forming a specified intensity profile of laser radiation is the use of special phase optical elements or systems. At present, there are many analytical [9–11] and numerical [12] methods of calculating phase elements. Numerical methods are more universal because, unlike analytical methods, they allow one to solve complex nontrivial problems of formation of intensity profiles. Among the known numerical methods, we should point out the iterative Gerchberg–Saxton algorithm [13], which has a number of advantages, namely, a simple implementation and a sufficiently high speed and accuracy. According to this algorithm, the phase function of an optical element is calculated from transverse intensity distributions specified in particular (input and output) planes of the system. A detailed scheme of the algorithm is given in Section 2 of this paper. However, the method for calculating the phase function by this algorithm was initially designed for single-mode laser radiation and the calculation mechanism for multimode radiation was not developed. In papers published to date [12, 14, 15], the Gerchberg–Saxton algorithm was used to reconstruct the phase function of only single-mode radiation, and there are no examples of application of this algorithm for multimode radiation. Therefore, the aim of this paper is to develop a universal method to control the intensity profile of transverse-multimode emission based on the Gerchberg–Saxton algorithm.

## 2. Experimental realisation of the Gerchberg–Saxton algorithm for the formation of transverse single-mode radiation

The Gerchberg–Saxton algorithm for calculating the phase function traditionally consists of the following basic steps [13] (Fig. 1).

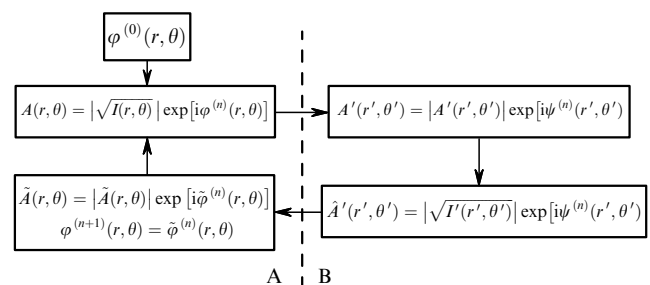


**Figure 1.** Scheme for solving the phase reconstruction problem by the Gerchberg–Saxton algorithm. A and B are the input and output planes.

(i) For the phase  $\varphi^{(0)}(r, \theta)$ , chosen as the initial approximation, and the given absolute field amplitude distribution  $|A(r, \theta)| = \sqrt{I(r, \theta)}$  in the input plane, one calculates the complex amplitude  $A'(r', \theta')$  in the output plane (here,  $r$  and  $\theta$  are the radius vector and the azimuthal angle in the input plane and  $r'$  and  $\theta'$  are the same parameters in the output plane). The conditions for the beam propagation from the input to the output plane are assumed to be known.

(ii) The modulus of the field amplitude calculated in the output plane is replaced by the square root of the desired intensity distribution  $I'(r', \theta')$  in this plane.

(iii) The backward beam propagation from the output to the input plane is calculated.

(iv) The calculated amplitude in the input plane  $\tilde{A}(r, \theta)$  is replaced by the square root of the given intensity distribution in the input plane and the calculated phase  $\tilde{\varphi}^{(n)}(r, \theta)$  is taken as the next approximation,  $\varphi^{(n+1)}(r, \theta) = \tilde{\varphi}^{(n)}(r, \theta)$ .

Then, the iteration procedure is repeated. As a rule, as a parameter characterising the algorithm convergence, one chooses the root-mean-square deviation of the intensity distribution calculated in the output plane from the required distribution. According to Parseval's theorem [12], the root-mean-square error should gradually decrease with increasing the number of iterations, and the calculated intensity distribution  $|A'^{(n)}(r', \theta')|^2$  should reach the required distribution  $I'(r', \theta')$ .

We used the Gerchberg–Saxton algorithm to experimentally form specified intensity distributions of laser radiation by a liquid-crystal (LC) modulator. Such modulators are currently widely used to control and correct laser radiation [16, 17]. They can serve as a base for creating controllable lenses [18], prisms [19], and diffraction gratings. In experiments on the formation of single-mode laser beams, we used an electrically controlled Holoeye-SLM-LC-2002 modulator (Fig. 2). This modulator is a phase optical element, which can change the wave-front phase of the propagating laser beam and consists of a liquid crystal placed between transparent electrodes [20]. One electrode of the modulator is solid and the other consists of a set of transparent electrodes–cells. The LC modulator is controlled by a VGA or SVGA video signal, which is transformed into an electric signal with the use of a special control unit. The black point of the control video signal corresponds to the minimum phase delay of the LC cell, and the white point corresponds to the maximum delay. The

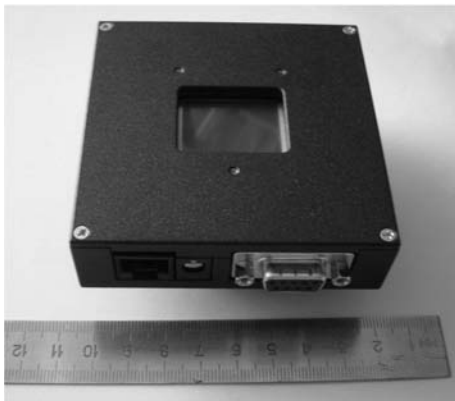


Figure 2. A Holoeye-SLM-LC-2002 modulator.

specification and the technical characteristics of the modulator used are as follows:

LC display .....	SONY LCX016AL-6
Panel size/mm .....	26.6 × 20.0 (1.3")
Resolution/pixels .....	832 × 624
Pixel pitch/μm .....	32
Maximum image frame rate/Hz .....	60
Maximum phase delay .....	$2\pi$ at $\lambda = 532$ nm
Filling factor .....	85 %
Overall dimensions/mm .....	82 × 82 × 23
Phase resolution .....	256 pixels (8 bit)
Display format .....	VGA, SVGA

The scheme of the experimental setup used to form specified intensity distributions is shown in Fig. 3. A diode laser beam ( $\lambda = 0.65$  μm) propagates through an expanding telescope ( $10\times$ ) and a LC modulator and is focused by a lens ( $f = 0.35$  m) on a CCD camera array. The LC modulator and the CCD camera array are placed in the focal planes of the lens. Hence, the distributions of the complex field amplitude in the plane of the LC modulator  $A(r, \theta)$  (plane A in Fig. 3) and on the CCD camera array  $A'(r', \theta')$  (plane B) are related by the Fourier transform. The field amplitude distribution  $|A(r, \theta)| = \sqrt{I(r, \theta)}$  in the plane A is known, and the desired intensity distribution in the plane B is given as  $|\hat{A}(r', \theta')| = \sqrt{I'(r', \theta')}$ . Applying the Gerchberg–Saxton algorithm to the scheme shown in Fig. 1, we can calculate the beam phase profile in the plane A corresponding to the phase delay introduced by the LC modulator and needed to form the required intensity distribution in the plane B. Some examples of intensity distributions obtained by this way on the CCD camera are shown in Fig. 4.

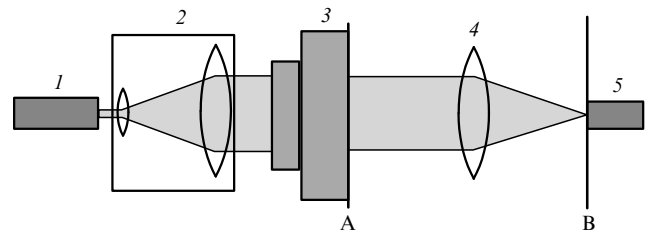
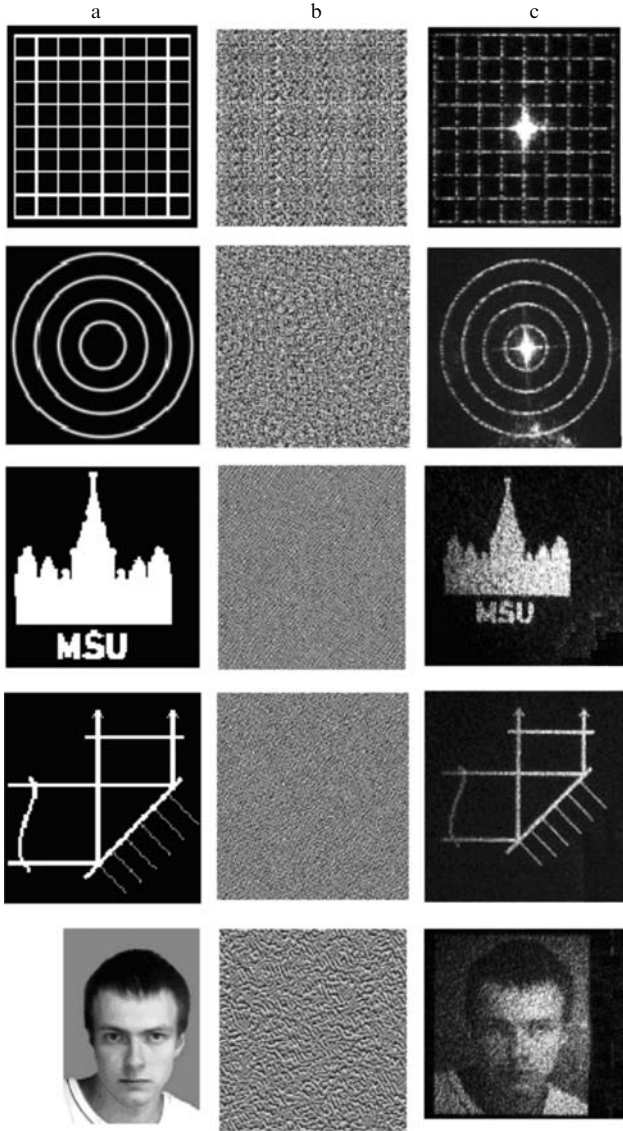


Figure 3. Scheme of the experimental setup for forming specified intensity distributions: (1) laser; (2) expanding telescope; (3) LC modulator; (4) lens; (5) CCD camera.

The above experiment demonstrates how the traditional Gerchberg–Saxton algorithm can be used to transform transverse-single mode laser radiation. However, as mentioned above, many technological processes require the use of multimode lasers.

### 3. Application of the Gerchberg–Saxton algorithm in the case of multimode radiation

Before discussing the formation of a specified intensity distribution, let us assume that we deal with a transverse multimode radiation coupled out of a stable laser resonator through a Brewster window. We assume that the transverse modes do not interfere due to the difference in their frequencies (the frequency degeneracy of the  $TEM_{01}$  and  $TEM_{10}$  modes is eliminated by an astigmatism introduced



**Figure 4.** Given intensity distributions (a), calculated grey scale (0 is black and 255 is white) phase distributions of the LC transparent (b), and obtained intensity distributions (c).

into the cavity by the Brewster window [21, 22]). Hence, in what follows, we consider the multimode radiation intensity as a sum of intensities of individual modes.

Let us elucidate the proposed modified algorithm of formation of multimode radiation in the focal plane of a lens on the example of a super-Gaussian beam with the intensity distribution

$$I'(r', \theta') = I'_0 \exp \left[ -2 \left( \frac{r'}{w'} \right)^{2p} \right] \quad (1)$$

(where  $I'_0$  is the peak intensity in the origin of coordinates of the output plane;  $w'$  is the characteristic beam size determined at the level of  $e^{-2}$  of the peak intensity; and  $p = 3$ ) formed from a beam summed of two transverse cavity modes with the intensity distribution

$$I_1(r, \theta) = 0.4E_{00}^2 + 0.6|E_{01}|^2 \quad (2)$$

or of four transverse cavity modes with the intensity distribution

$$I_2(r, \theta) = 0.15E_{00}^2 + 0.35|E_{01}|^2 + 0.15E_{10}^2 + 0.35|E_{02}|^2. \quad (3)$$

Here,  $E_{00}$ ,  $E_{01}$ ,  $E_{10}$ , and  $E_{02}$  are the amplitudes of transverse cavity modes  $\text{TEM}_{00}$ ,  $\text{TEM}_{01}$ ,  $\text{TEM}_{10}$ , and  $\text{TEM}_{02}$ , respectively, which can be written in the form [1, 23]

$$E_{00}(r, \theta) = E_0 \exp(-\rho^2/2);$$

$$E_{01}(r, \theta) = E_0 \exp(-\rho^2/2) \exp(i\theta);$$

$$E_{10}(r, \theta) = E_0(1 - \rho^2) \exp(-\rho^2/2);$$

$$E_{02}(r, \theta) = E_0 \rho^2 \exp(-\rho^2/2) \exp(i2\theta);$$

where  $E_0$  is the field amplitude in the beam centre;  $\rho = r\sqrt{2}/w$ ; and  $w$  is the characteristic size of the  $\text{TEM}_{00}$  mode. The numerical coefficients in expressions (2) and (3) characterise the power ratios of modes in the beam and are chosen arbitrarily.

The numerical calculations were performed for a model optical scheme similar to the experimental scheme shown in Fig. 3. We assume that the field  $A(r, \theta)$  in the input plane A and the field  $A'(r', \theta')$  in the output plane B are related by an integral relation that is more universal than the Fourier transform and allows one, if necessary, to position the A and B planes at distances  $L_1$  and  $L_2$  that need not be equal to the focal distance  $f$  of lens (4). This integral relation has the form

$$A'(r', \theta') = \frac{\exp(ikz)}{i\lambda f} \int_0^{2\pi} d\theta \int_0^{R_0} \exp \left\{ \frac{ik}{2B} [Dr'^2 + Ar^2 - 2r'r \cos(\theta - \theta')] \right\} |A(r, \theta)| \exp[i\varphi(r, \theta)] r dr, \quad (4)$$

where  $k$  is the wave number;  $\lambda$  is the radiation wavelength;  $z$  is the distance between the planes;  $R_0$  is the radius of the input aperture; and  $A$ ,  $B$ , and  $D$  are the elements of the  $ABCD$  beam matrix, which, for the given scheme, are  $A = 0$ ,  $B = f$ , and  $D = 1 - (L_1/f)$ .

The steps 1–4 of the iterative algorithm were performed according to the scheme shown in Fig. 1. At the first iteration, we gave an initial plane-phase approximation for each mode and calculated their propagation to the input to the output plane. The transverse amplitude distribution for each mode in the output plane was replaced by the square root of the desired intensity distribution with a corresponding weight coefficient that characterises the percentage of the mode power in the radiation. The phase of each mode calculated in the output plane was unchanged. Then, we calculated the backward propagation of modes and replaced the calculated mode amplitudes in the input plane  $\tilde{A}_i^{(n)}(r, \theta)$  by the known amplitudes. The phase profile  $\varphi_i^{(n)}(r, \theta)$  of the  $i$ th mode was calculated by the expression

$$\varphi_i^{(n)}(r, \theta) = \arctan \frac{\text{Im}[\tilde{A}_i^{(n)}(r, \theta)]}{\text{Re}[\tilde{A}_i^{(n)}(r, \theta)]}.$$

The difference between our and traditional algorithms is that, next to  $\varphi^{(0)}$ , we calculate  $\varphi^{(n+1)}(r, \theta)$  phase approximations in the input plane, which are needed to form a required intensity distribution. We suggest to calculate the new phase approximation  $\varphi_i^{(n+1)}(r, \theta)$  based on the following empirical consideration: the effect of a phase element on the mode propagation is maximum in the beam points where the mode intensity is maximum. Thus, the new phase approximation (phase function)  $\varphi^{(n+1)}(r, \theta)$  at the  $(n+1)$  iteration, which is similar for all modes, is determined by the expression

$$\varphi^{(n+1)}(r, \theta) = \sum_{i=1}^N \alpha_i(r, \theta) \varphi_i^{(n)}(r, \theta), \quad (5)$$

where  $\alpha_i(r, \theta) = I_i(r, \theta) / \sum_{i=1}^N I_i(r, \theta)$ ;  $i = 1, \dots, N$ ;  $N$  is the number of modes in the initial beam,  $I_i(r, \theta)$  is the  $i$ th mode intensity; and  $\varphi_i^{(n)}(r, \theta)$  is the phase of the  $i$ th mode calculated at the  $n$ th iteration. We assumed that the wave front calculated by this method was reproduced at each iteration by an ideal phase transparent (i.e., the reproducibility error was zero).

It is necessary to note that the vortex component of the phase distribution of the  $\text{TEM}_{01}$  and  $\text{TEM}_{02}$  modes remained constant: for calculating a new approximation of the corrector phase, the  $\text{TEM}_{01}$  and  $\text{TEM}_{02}$  modes were introduced into expression (5) without vortex components.

As a parameter characterising both the algorithm convergence and the error in the formation of a specified intensity distribution, we chose the deviation of the intensity distribution formed in the output plane from the desired distribution,

$$\Delta I^{(n)} = \int_0^{2\pi} d\theta' \int_0^{R_1} \left\{ I'(r', \theta') - \sum_{i=1}^N [A_i'^{(n)}(r', \theta')]^2 \right\}^2 r' dr' \times \left\{ \int_0^{2\pi} d\theta' \int_0^{R_1} [I'(r', \theta')]^2 r' dr' \right\}^{-1}, \quad (6)$$

where  $R_1$  is the output aperture radius and  $\sum_{i=1}^N [A_i'^{(n)}(r', \theta')]^2$  is the multimode beam intensity distribution obtained at the  $n$ th iteration of the Gerchberg–Saxton algorithm.

As functional (6) reaches the minimum or a predetermined small value, we consider that the wave front needed to form radiation is calculated and can be reproduced by a real phase element. In our case, such an element was an 18-electrode semipassive bimorph flexible mirror [24, 25], whose parameters (response function) were used for numerical simulation. In the simulation, we used a scheme that was similar to the scheme shown in Fig. 3 with a bimorph mirror instead of the LC modulator in the plane A. The mirror design and the configuration of its electrodes are shown in Fig. 5. The mirror surface profile can be represented in the form

$$F(r, \theta) = \sum_{k=1}^K V_k \Phi_k(r, \theta), \quad (7)$$

where  $V_k$  is the voltage at the  $k$ th electrode;  $K = 18$  is the number of electrodes; and  $\Phi_k(r, \theta)$  is the response function of the  $k$ th electrode (as the response function, we use the mirror surface deformation caused by the action of only one control drive). For convenience, the mirror response

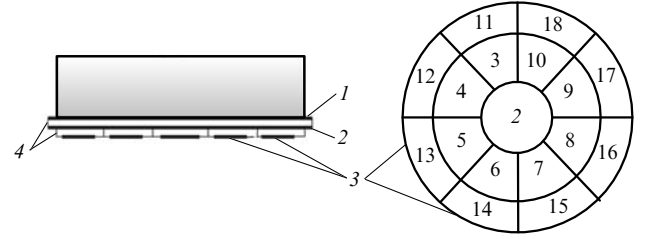


**Figure 5.** Construction of the bimorph flexible mirror and configuration of its electrodes: (1) focusing/defocusing electrode; (2) common ground electrode; (3) segmented electrodes; and (4) piezoceramic discs.

functions were represented in the form of the Zernike polynomial expansion. The functional characterising the error of reproducibility of the calculated wave front  $\varphi(r, \theta)$  by the bimorph flexible mirror has the form

$$J = \int_0^{2\pi} d\theta \int_0^{R_0} \left[ \varphi(r, \theta) - \sum_{k=1}^K V_k \Phi_k(r, \theta) \right]^2 r dr, \quad (8)$$

where  $R_0$  is the mirror radius equal to the radius of the input aperture.

Thus, the calculation of required control voltages at the electrodes is reduced to the minimisation of the functional  $J$ , i.e. to the determination of such voltages  $V_k$  for which all the partial derivatives become zero,  $\partial J / \partial V_k = 0$ .

#### 4. Algorithm convergence and the main results

It is known that, when using the Gerchberg–Saxton algorithm, even small variations in the characteristics of the chosen optical system or in the laser radiation parameters can significantly affect the formation error. In this connection, it was necessary to find a parameter responsible for the algorithm convergence and for the achievable formation error. As such a parameter, we suggest to use the parameter  $\beta$  that takes into account the characteristics of the laser radiation and optical system,

$$\beta = \frac{\pi w_0 w'}{f \lambda}, \quad (9)$$

where  $w_0$  is the characteristic beam size in the input plane determined at the level of  $e^{-2}$  of the peak intensity and  $w'$  is the characteristic beam size to be obtained in the output plane (at the level of  $e^{-2}$ ). As follows from the definition, under certain conditions, the chosen parameter  $\beta$  becomes similar to the so-called beam quality factor  $M^2$  [26]. Similar to the parameter  $\beta$ , the  $M^2$  factor is calculated by expression (9) with the only difference that the characteristic beam size  $w'$  in the output plane is real instead of desired. In the cases when the real beam size coincides with the beam size to be obtained, as, for example, in the case of successful realisation of the Gerchberg–Saxton algorithm, the  $\beta$  parameter can be considered to be identical to the  $M^2$  factor.

One more advantage of the  $\beta$  parameter is that, having calculated the phase function for a particular optical system, we can assert that this function will be the same for an optical system that has a different geometry and beam parameters in the input and output planes but the same  $\beta$  parameter as the initial system [27].

**Table 1.** Gerchberg–Saxton algorithm convergence as a function of the  $\beta$  parameter.

Two-mode initial radiation		Four-mode initial radiation	
$\beta$	$\Delta I^{(n)}$ (%)	$\beta$	$\Delta I^{(n)}$ (%)
2.20	5	2.64	2.8
2.55	9	3.05	1.5
2.93	8.6	3.52	6.2
4.00	8.2	3.96	10
4.37	8.2	4.40	8.8
5.10	7.9	4.85	9.3
5.83	8.6	5.28	12.1
6.55	8.9	5.72	11.2
6.93	10.8	6.16	11.9
7.30	14.7	6.60	12.8
8.37	16.6	7.00	13.9
9.05	13.6	7.44	14.6
9.46	18.6	7.90	16.8
10.20	23	8.33	19.9
10.52	23.1	9.20	20.4

We analysed the accuracy of formation of a beam with the super-Gaussian intensity distribution from beams given by expressions (2) and (3) as a function of the  $\beta$  parameter. To change  $\beta$ , we changed the initial beam size  $w_0$ . The other values that determine the  $\beta$  parameter were constant. Table 1 lists the formation errors  $\Delta I^{(n)}$  at the last iteration (after which the solution accuracy ceases to improve) for different  $\beta$  parameters in the case of two- and four-mode

initial radiation. One can see that the best result for the two-mode beam was obtained at  $\beta = 2.2$ . This corresponds to the following calculation parameters:  $\lambda = 1.06 \mu\text{m}$ ,  $L_1 = 5 \text{ m}$ , and  $L_2 = f = 0.45 \text{ m}$ . The characteristic beam sizes  $w_0$  and  $w'$  in the input and output planes were, respectively, 8.3 and 0.4 mm with  $R_0 = 15 \text{ mm}$  and  $R_1 = 0.9 \text{ mm}$ . The minimum error (5 %) of the formation by an ideal corrector was achieved at the tenth iteration. The intensity distribution to be formed and the intensity profiles obtained in the output plane before and after using the Gerchberg–Saxton algorithm are shown in Figs 6a, b. The results of numerical simulation of formation of the given transverse intensity distribution by a bimorph flexible mirror and the corresponding shape of the mirror surface are given in Figs 6c, d. The error in the reproducibility of the given phase profile by the mirror was 0.5 %. The error in the formation of the given intensity distribution by the bimorph mirror was 5.3 %.

The best formation result for the four-mode beam was achieved at  $\beta = 3.05$ . The error in the intensity distribution formation decreases from 17 % at the first iteration to 1.5 % after 20 iterations. The error of reproducibility of the given phase distribution by the flexible mirror was 1.5 %. In this case, the error in the formation of a beam with the super-Gaussian intensity profile by the bimorph mirror was 1.6 %. The calculation parameters of the beam and optical scheme were as follows:  $\lambda = 1.06 \mu\text{m}$ ,  $L_1 = 5 \text{ m}$ ,  $L_2 = f = 0.45 \text{ m}$ ,  $R_0 = 20 \text{ mm}$ ,  $R_1 = 0.9 \text{ mm}$ ,  $w_0 = 11.6 \text{ mm}$ , and  $w' = 0.4 \text{ mm}$ . The desired intensity distribution and the beam intensity profiles obtained in the output plane before and

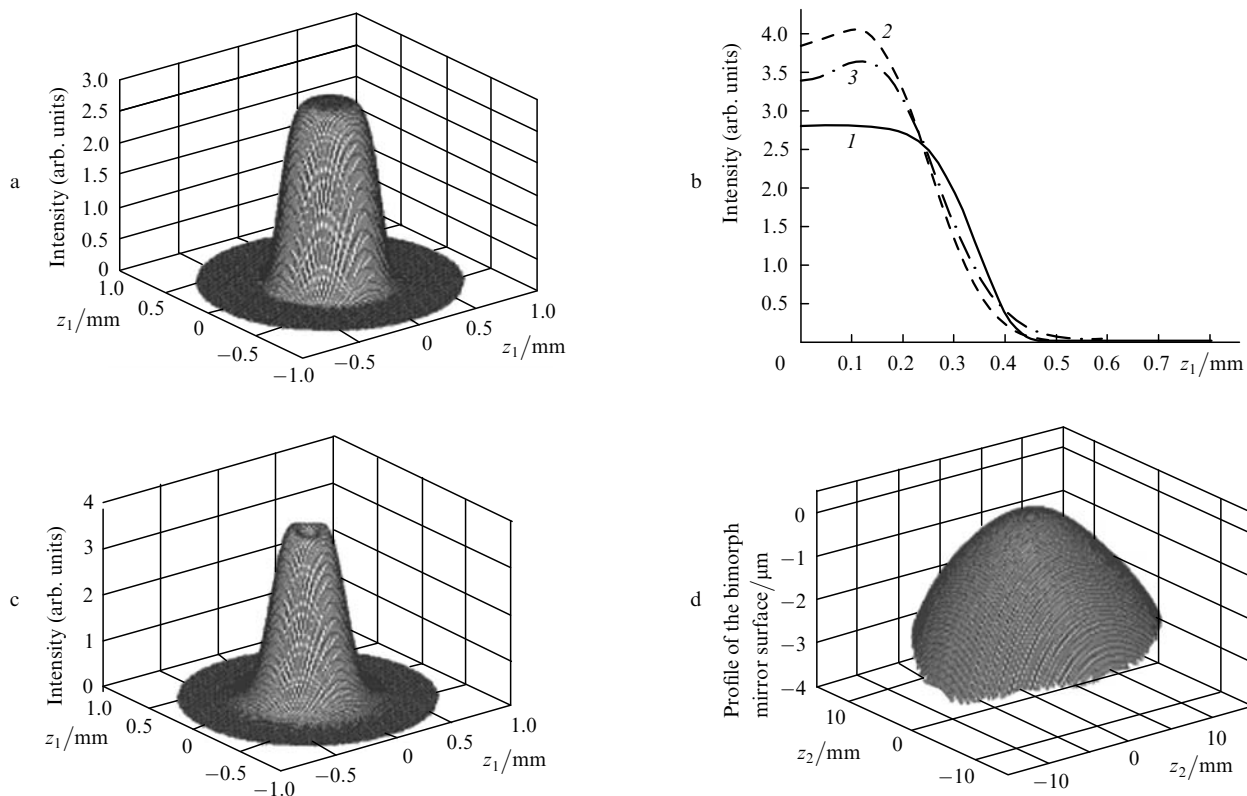


**Figure 6.** Formation of the third-order super-Gaussian intensity distribution from two-mode radiation: required intensity distribution (a); required intensity profile ( $I$ ) and profiles obtained before (2) and after (3) using the Gerchberg–Saxton algorithm with the help of an ideal corrector (b); intensity distribution formed by a bimorph mirror (c); and shape of the bimorph mirror surface (d) ( $z_1$  is the distance from the output aperture centre and  $z_2$  is the distance from the input aperture centre).

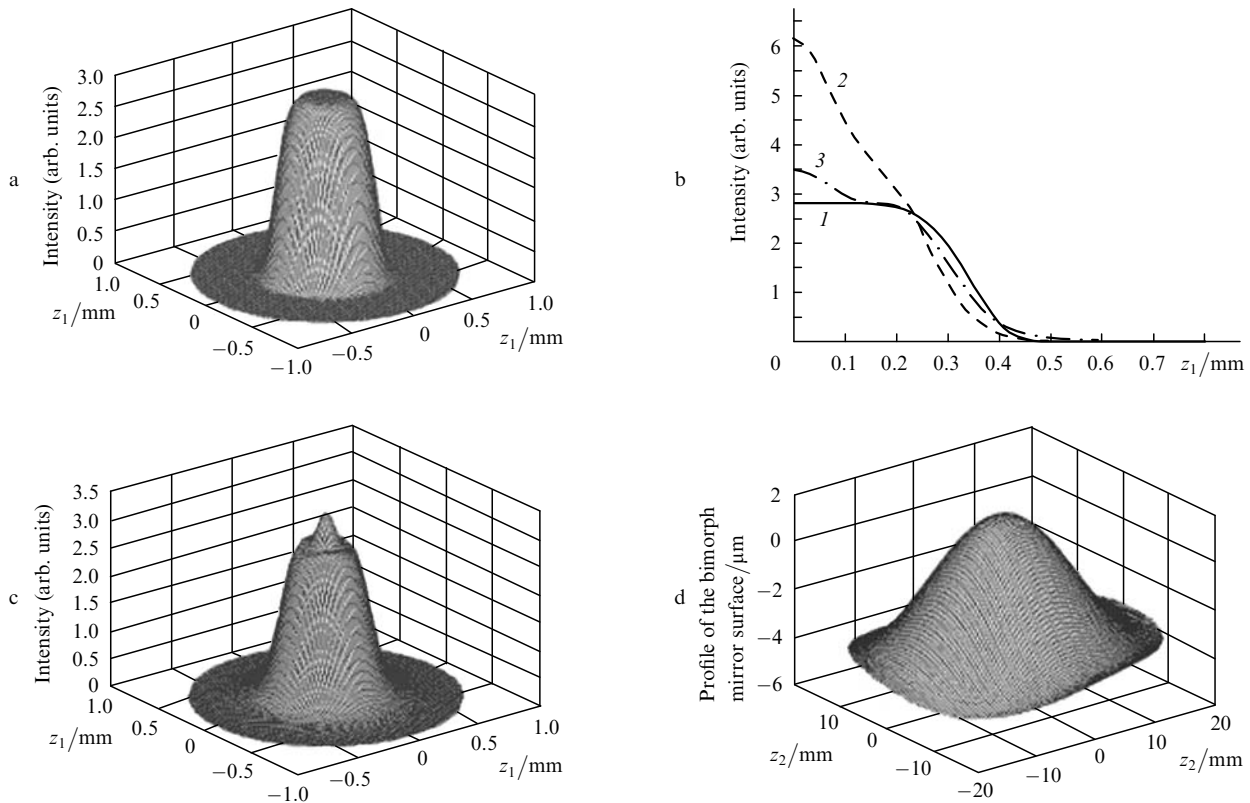


**Figure 7.** Formation of the third-order super-Gaussian intensity distribution for four-mode radiation: required intensity distribution (a); required intensity profile ( $I$ ) and profiles obtained before (2) and after (3) using the Gerchberg–Saxton algorithm with the help of an ideal corrector (b); intensity distribution formed by a bimorph mirror (c); and shape of the bimorph mirror surface (d) ( $z_1$  is the distance from the output aperture centre and  $z_2$  is the distance from the input aperture centre).

after application of the Gerchberg–Saxton algorithm with the use of an ideal corrector are shown in Figs 7a, b. The intensity distribution obtained in the output plane with the use of the bimorph mirror (numerical simulation) and the mirror surface shape are shown in Figs 7c, d.

It should be noted that there are limits ( $\beta = 2.20$  in the case of two-mode beams and  $\beta = 2.64$  for four-mode beams) below which the formation problem cannot be solved. The absence of the algorithm convergence in these cases is explained by the impossibility to focus the beam into a spot smaller than diffraction-limited for a given beam.

## 5. Conclusions

In this paper, we have experimentally demonstrated the formation of various specified intensity distributions using the Gerchberg–Saxton algorithm. A modified scheme of this algorithm is proposed to solve the problem of formation of required intensity distributions in the case of transverse-multimode laser beams. The formation of beams with the super-Gaussian intensity distribution from beams composed of two ( $TEM_{00}$  and  $TEM_{01}$ ) or four ( $TEM_{00}$ ,  $TEM_{01}$ ,  $TEM_{10}$  and  $TEM_{02}$ ) transverse cavity modes is numerically simulated. A flexible bimorph mirror has been used as a phase element. The smallest error in the formation of the super-Gaussian intensity distribution by the bimorph mirror is 5.3% and 1.6% in the case of two- and four-mode radiation, respectively. We have introduced a parameter  $\beta$  that allowed us to predict the error in the

formation of a given intensity profile, as well as the Gerchberg–Saxton algorithm convergence on the whole.

**Acknowledgements.** The authors thank A.Y. Kostylev for his help in experiments with the LC transparent.

## References

1. Steen W.M. *Laser Material Processing* (London: Springer-Verlag, 2003).
2. Webb C.E., Jones J.D.C. *Handbook of Laser Technology and Applications* (Bristol, Philadelphia: Institut of Physics Publ., 2004) Vol. 3, p. 1557.
3. Azar D.T., Koch D.D. *LASIK Fundamentals, Surgical Techniques, and Complications* (New York: Marcel Dekker Inc., 2002).
4. Bliss E.S., Peterson R.L., Salmon J.T., Thomas R.A. *Proc. SPIE Int. Soc. Opt. Eng.*, **1859**, 130 (1993).
5. Forbes A., Botha L., in *Laser Beam Shaping Applications* (Boca Raton, Fla: CRC Press, 2006) p. 183.
6. Boreisho A.S. *Lasery: ustroystvo i deystvie* (Lasers: Design and Operation) (St. Petersburg: Mekh. Institute, 1993).
7. Abil'siitov G.A. *Tekhnologicheskie lasery* (Technological Lasers) (Moscow, Mashinostroenie, 1991) Vol. 1.
8. Koebner H. *Industrial Applications of Lasers* (New York: Wiley-Interscience, 1988).
9. Woods S.C., Greenaway A.H. *J. Opt. Soc. Am. A*, **20**, 508 (2003).
10. Campbell H.I., Zhang S., Restaino S., Greenaway A.H. *Opt. Lett.*, **29**, 2707 (2004).
11. Romero L.A., Dickey F.M. *J. Opt. Soc. Am. A*, **13**, 751 (1996).
12. Fienup J.R. *Appl. Opt.*, **21**, 2758 (1982).
13. Gerchberg R.W., Saxton W.O. *Optic (Stuttgart)*, **34**, 227 (1972).

14. Courtial J., Whyte G., Bouchal Z., Wagner J. *Opt. Express*, **14**, 2108 (2006).
15. Liu J.S., Caley A.J., Taghizadeh M.R. *Opt. Commun.*, **267**, 347 (2006).
16. Restaino S., Dayton D., Browne S., Gonglewski J., Baker J., Rogers S., Mcdermott S., Gallegos J., Shilko M. *Opt. Express*, **6**, 2 (2000).
17. Dayton D., Sandven S., Browne S., Gonglewsky J., Rogers S., Mcdermott S. *Opt. Express*, **1**, 338 (1997).
18. Naumov A.F., Loktev M.Yu., Guralik I.R., Vdovin G. *Opt. Lett.*, **23**, 992 (1998).
19. Vasil'ev A.A., Kompanets I.N., Parfenov A.V. *Kvantovaya Elektron.*, **10**, 1079 (1983) [*Sov. J. Quantum Electron.*, **13**, 689 (1983)].
20. Vorontsov M.A., Koryabin A.V., Shmalhausen V.I. *Upravlyaemye opticheskie sistemy* (Controlled Optical Systems) (Moscow: Nauka, 1988).
21. Siegman A.E. *Lasers* (Mill Valley, CA: University Science Books, 1986) p.690.
22. Louvergeneaux E., Hennequin D., Dangoisse D., Glorieux P. *Phys. Rev. A*, **53**, 4435 (1996).
23. Anan'ev Yu.A. *Opticheskie resonatory i lasernye puchki* (Optical Resonators and Laser Beams) (Moscow: Nauka, 1990).
24. Kudryashov A., Shmal'hausen V.I. *Opt. Eng.*, **35**, 3064 (1996).
25. Cherezova T.Yu., Kaptsov L.N., Kudryashov A.V. *Appl. Opt.*, **35**, 2554 (1996).
26. Sheldakova J., Cherezova T., Alexandrov A., Rukosuev A., Kudryashov A. *Proc. SPIE Int. Soc. Opt. Eng.*, **5708**, 352 (2005).
27. Dickey F.M., Holswade S.C., in *Laser Beam Shaping Applications* (Boca Raton, Fla: CRC Press, 2006) p.269.